Wave Induced Stresses Measured at the Wave Dragon Nissum Bredning Prototype

Corona, L.; Kofoed, Jens Peter

Published in:
Proceedings of the Third CA-OE Workshop

Publication date:
2006

Document Version
Publisher's PDF, also known as Version of record

Wave induced stresses measured at the Wave Dragon Nissum Bredning Prototype

L.Corona [1,2] , J.P. Kofoed [1]

[1] *Department of Civil Engineering, Aalborg University*
[2] *Institut Supérieur de l'Automobile et des Transports (ISAT), 58000 Nevers*
mail : corona_loic@yahoo.fr

Abstract

The paper describes the wave induced loading on the overtopping based wave energy converter Wave Dragon. Focus is put on the junction between the main body and the reflector, also called the "shoulder part", where large cross sectional forces and bending moments acts.

There are two main objectives for this paper, first to verify the FEM results obtained by Niras, Danish society in charge of the finite element modelling and structural design, and then to make a first experimental fatigue analysis of a particular part of the Wave Dragon. This last part shall be considered as an exercise for the further work that is to be done for the fatigue analysis, and which is not part of this paper.

Introduction

A prototype of the Wave Dragon has been tested in real sea for almost two years in Nissum Bredning, Denmark. The prototype is a scale down (length scale 1:4.5) of a 4 MW North Sea production plant. The structure has been equipped with a total of 108 strain gauges (36 rosettes) including 8 rosettes located in the shoulder part of the main body. Their aim has been to monitor forces in the structure induced by the interaction between the main body and the reflector.

The readings from the strain gauges have been registered through out the year 2004. A subset of these data has been analyzed into details. The selected data covers a wide range of sea states.

The spectra of the analysed strains and stresses will then be used twice. Firstly, the strains measured will be correlated with the FE results in our possession. Secondly, an experimental fatigue analysis will be done, on a particular part of the main body.

Such results provides a basis for calibration of a finite element model of the Wave Dragon structure and offers a possibility of minimizing the uncertainty on the estimation of the loads acting on the structure, enabling an optimized structural design and thereby reduction in cost.

EXPERIMENTAL CONFIGURATION

PRESENTATION

WD consists of three main elements (see Fig.1):

- Two patented wave reflectors focusing the waves towards the ramp, linked to the main structure. The wave reflectors have the verified effect of increasing the significant wave height substantially and thereby increasing energy capture by 70 % in typical wave conditions.
- The main structure consisting of a patented doubly curved ramp and a water storage reservoir.
- A set of low head propeller turbines for converting the hydraulic head in the reservoir into electricity.

When waves have been focused by the reflectors they overtop the ramp and fill the reservoir, which is situated at a higher level than the surrounding sea. This hydraulic head is utilized for power production through the hydro turbines.

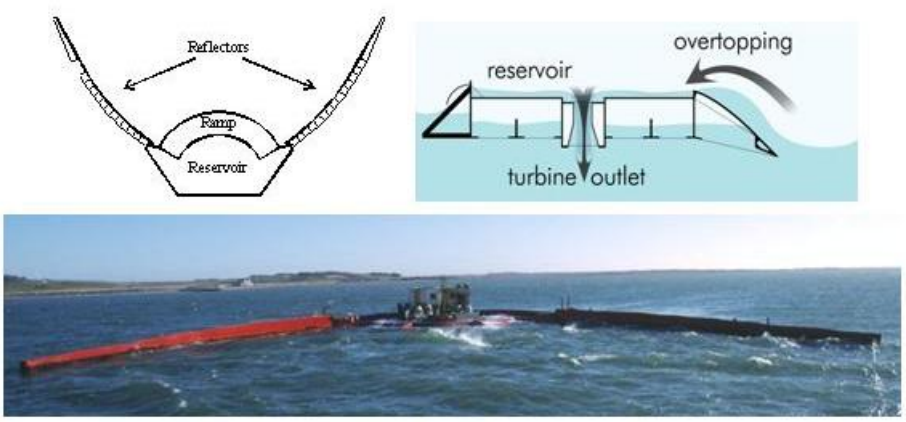

Figure 1: *Top left:* Main components of the WD. *Top right:* The basic principle of the WD *Below:* WD prototype at test site.

Strain gauges have been placed on different part of the Wave Dragon. Figure 2 shows the positions of those gauges (the positions shown here are mirrored). The 24 gauges here considered are numbered from 41 to 64 on this drawing. See also [5] for more detailed pictures.

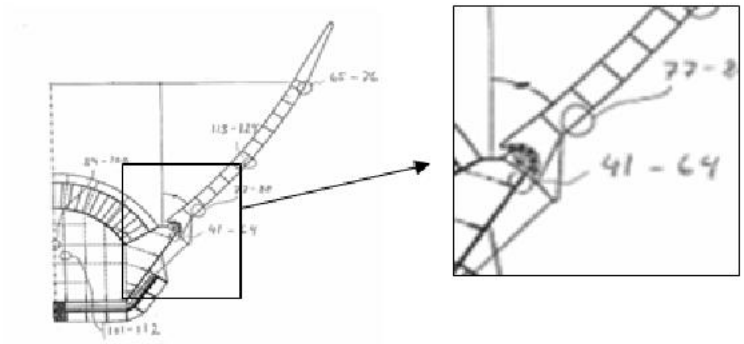

Figure 2: SG positions

Due to an incident, water has been introduced for a little while in the buoyancy tank where the strain gauges are situated. Even if the problem is totally solved now, the salt water has altered some gauges at the shoulder part.

CONFIGURATION OF THE GAUGES

The gauges are used in rosettes, with a 45 degree angle between each gauge, as shown on the figure 3, where **x** is the direction of the reflector.

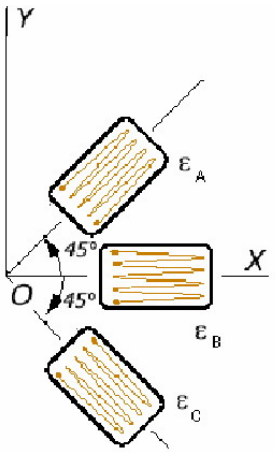

Figure 3: Rosette configuration

These rosettes are placed inside a buoyancy tank, near the shoulder junction, on the port side of the device. Six of those rosettes are placed on the vertical wall, one on the top and one on the bottom of the compartment. The bottom and top y direction are the opposite.

The sample rate for data acquisition is 10Hz, and data have been recorded in 30 minutes files.

RESTRICTION FOR THE DATA OBTAINED FROM THE SG

As mentioned, some gauges have been influenced by contact with salt water, and so rust can exist between a gauge and the wall. In this case, the readings given by the gauges do not reflect the reality. Moreover, some wires can have been broken, or even some gauges.

Only the rosettes located on the vertical wall will be considered, because the stiffness of the top and bottom parts is much higher. Figure 4 shows the malfunctioning gauges on black, on the vertical wall.

Moreover, considerable noises are present in the recorded signal. A portion of this noise comes from electrical problems, and also moisture can affect the signal. The values obtained can be altered by other electrical phenomenon taking place on board. The temperature is also influencing the data. However, no temperature compensation has been applied, due to the lack of relevant information.

Another problem comes from the offset values for those gauges, which are unknown at the time of data acquisition. In fact, the gauges were installed while the device was still on shore, and the equilibrium position in buoyant condition is different from the initial one. As a consequence, neither the correct offsets, nor the average deviation between shore and sea states are correctly defined.

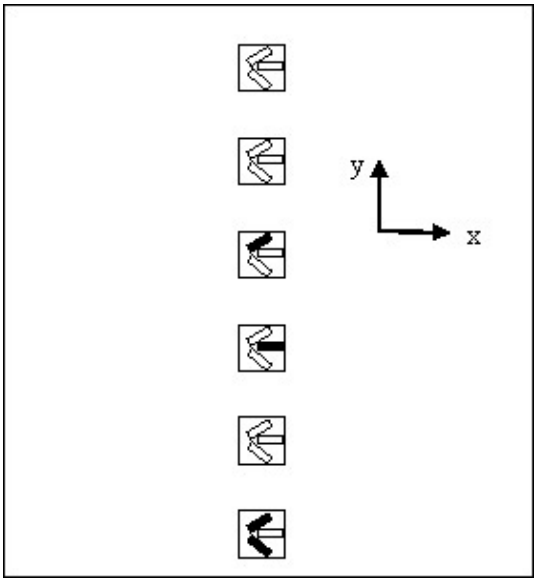

Figure 4: Malfunctioning gauges

PARASITE PHENOMENA IN RECORDED SIGNALS

JUMP IN THE TIME DOMAIN

As it can seen from figure 5, some files contains long periodic phenomenon. When looking in detail at these jumps, it can be seen that they represent very fast change in the signal. If they were physically induced, they should be the result of chock, with no progressive changes. But the junction between the reflector and the main body contain fender elements, so it is sure that this phenomenon does not reflect the reality.

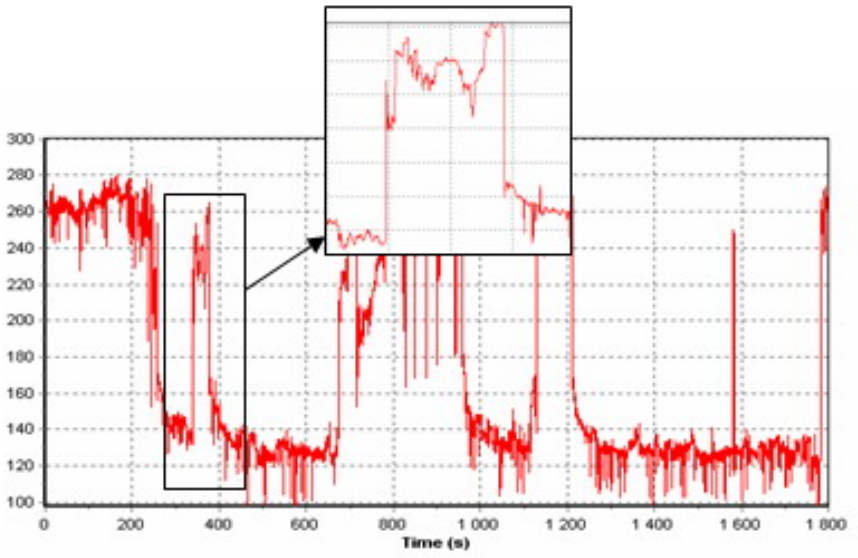

Figure 5: Long periodic jump

HIGH FREQUENCY

In some other data files, various high frequency phenomena exist (cf. Figure 6). In the analysis are defined as high frequency all phenomena with frequency higher than one second. Indeed it is assumed that phenomena quicker than three times the wave period are not reflecting reality. This is true, because here are measured the strains in the x direction, and even if

the plate vibrate, the membrane deviation induced will be very low. Moreover, it has been seen, while looking at a large number of data files, that the error induced by suppressing the harmonics of the response equal and larger than third order is relatively low. Therefore we will consider no high frequency phenomenon at all.

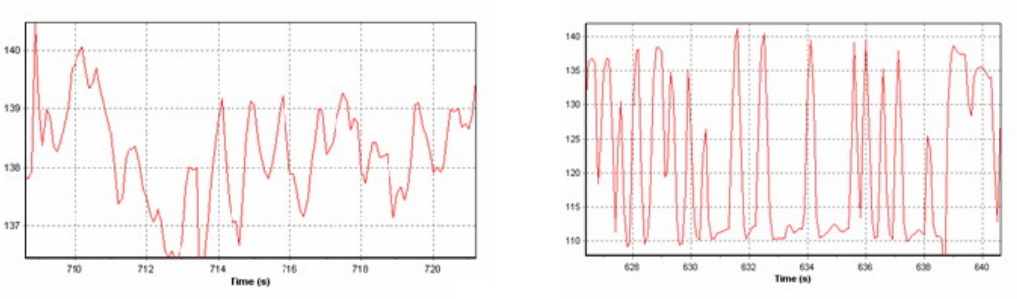

Figure 6: High Frequency Noise

LINEAR COMPONENT

The linear increase in time is supposed to be mainly induced by the temperature, and so don't reflect the physical stresses. Indeed, the increase of temperature changes the resistance of the gauges.

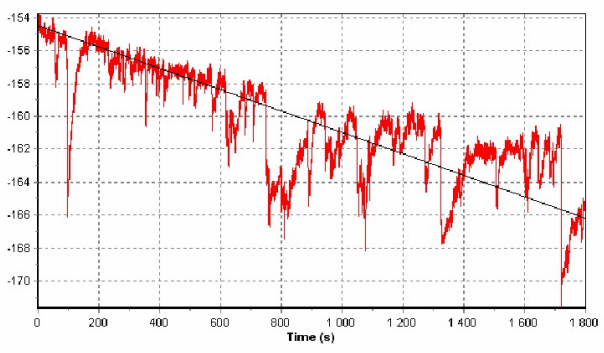

Figure 7: Linear component in the time domain

CONCLUSION

Due to the phenomena here described, finding relevant data, and extracting the meaningful components have been a hard nominal work. Also, a lot of data files have been disregarded, and focus has been put on the less noisy measurements. To be sure to extract the most important (and true) components, choice has been made to work with the Fast Fourier Transform (FFT) of the signal. Indeed, the FFT will lead to have the amplitude of strains deviation related to the frequency these phenomena appear, thus it will be easier to separate long periodic and wave induced phenomenon.

SPECTRAL ANALYSIS OF THE SIGNAL

The Wave Lab software, developed at Aalborg University, has been used for data processing. Indeed, several basic mathematic routines are easily available within this software. This software offers a FFT process for frequency domain analysis of the data, and also several possibilities for channel combination and simple data manipulation. The different settings used for the FFT will now be discussed, as well as the way to use the data.

BANDPASS FILTERING

When performing the FFT of the signal, it is possible to set low and high bandpass filter. To skip the average value, as well as very long periodic phenomenon, a low pass boarder has been set. As it has been explained before, the phenomena faster than one Hertz are disregarded, so the high pass filter is set at 1 Hz.

The surge movement of the structure is the longest phenomenon noticed due to other data. The period of this motion is around 100s, so a cut frequency is defined at 0.0033 Hz, corresponding to 300s.

NUMBER OF POINT IN THE FFT

The number of points used for the FFT, in each sub-series, affects the values obtained. Indeed, the frequency resolution increases with the number of data points used. In the opposite, the spectral value is more accurate while using fewer points (see Fig. 8). As we are limited by the number of data points available, if we use more points, then there are fewer Fourier data sets, and so fewer correlations between the spectral values.

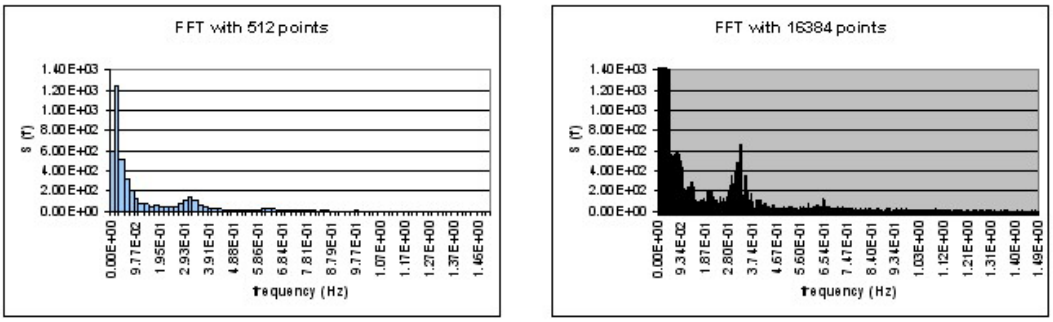

Figure 8: FFT of the same file, with a different number of points in each dataset

The total number of data points contained in one file is 18.000. So, to have a frequency resolution superior as the low cut frequency and to obtain at least 4 data sets for the FFT, it has been chosen to use 4096 points in each sub-series. The frequency resolution is then :

$$\Delta F = \frac{10}{4096} = 2.44 \times 10^{-3} Hz \tag{1}$$

DESCRIPTION OF THE CHOSEN ANALYSIS

In the spectrum of the different signals, it has been seen that there are roughly three main components. A long periodic component, which stand for the long periodic phenomena, and the two others are in the same frequency than waves (direct response) and twice this frequency (harmonic response). In this analysis, long periodic and wave related components will be separeted. As the Fourier transform is linear, it is possible to do so.

As the wave frequency is well defined, we will use it in our analysis. Thus it has been chosen a low cut frequency of a third and a high cut frequency of three times the wave frequency. This roughly corresponds to 0.1 Hz and 1 Hz respectively. Then spectral values of less than

0.1 Hz will be considered as long periodic variation, and spectral values of more than 1 Hz will be disregarded. Figure 9 shows an example of FFT obtained for a strain gauge.

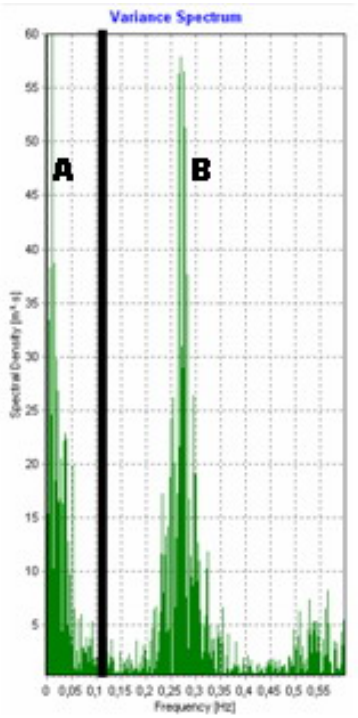

Figure 9: Standard spectrum of a strain gauge

Then, the m_0 moments for the different spectrum is calculated. This first order moment is equal to the area of histograms:

$$(m_0)_{long\_T} = \int_{0.0033}^{0.1} S(f).df = \sum S_i \Delta f_i \qquad , \forall i \in A \tag{2}$$

$$(m_0)_{wave} = \int_{0.1}^{1} S(f).df = \sum S_j \Delta f_j \qquad , \forall j \in B \tag{3}$$

The m_0 moment is representative for the variance of the signal. The strain deviation is defined as the squared root of m_0 :

$$\Delta\epsilon = \sqrt{m_0} \tag{4}$$

These spectral values will be related to the significant wave height, Hs. Hs is obtained trough a pressure transducer, and the appropriate analysis method. Those values are already calculated in an other data file.

Thus, for one data file of 30 minutes, the results of this analysis are a strain deviation related to the surge frequency and a strain deviation related to the wave frequency. These components will be related to the significant wave height during the measurement.

First, focus will only be put on the strain in the x direction, given by the axial gauge of each rosette. Then the stresses in the different directions will be discussed, and a model of fatigue analysis that is to be done for the Wave Dragon will be established. It's important to understand that this Fatigue analysis is not complete. Indeed, only the instrumented points of the structure are considered, and other "hotspots" are most likely present.

RESULTS FOR THE STRAIN IN THE X DIRECTION

Now will be presented the results obtained through the data analysis described before. As it has been said, it was difficult to find good results in the data files. After a first look at all the different results, the data files taken from the 17^{th} of November 2004 to the 24^{th} of November were selected. Here are presented the results obtained, considering all the data files, and also the time evolution of the sea state.

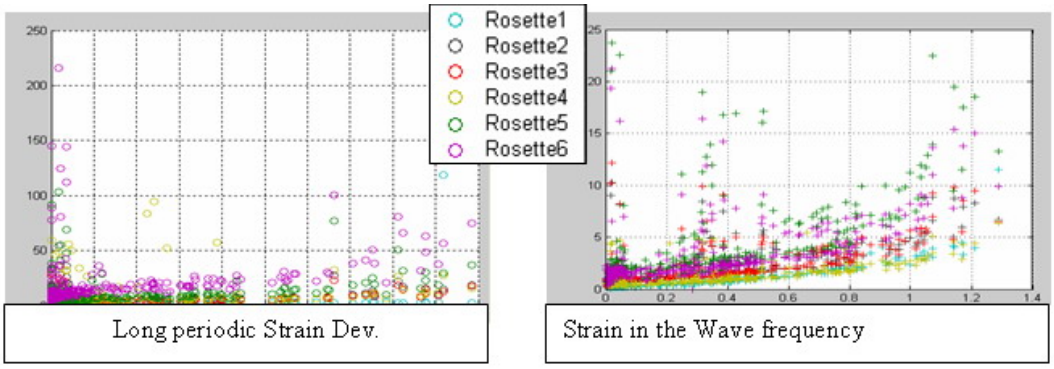

Figure 10: ϵ_{xx} obtained considering 336 following files

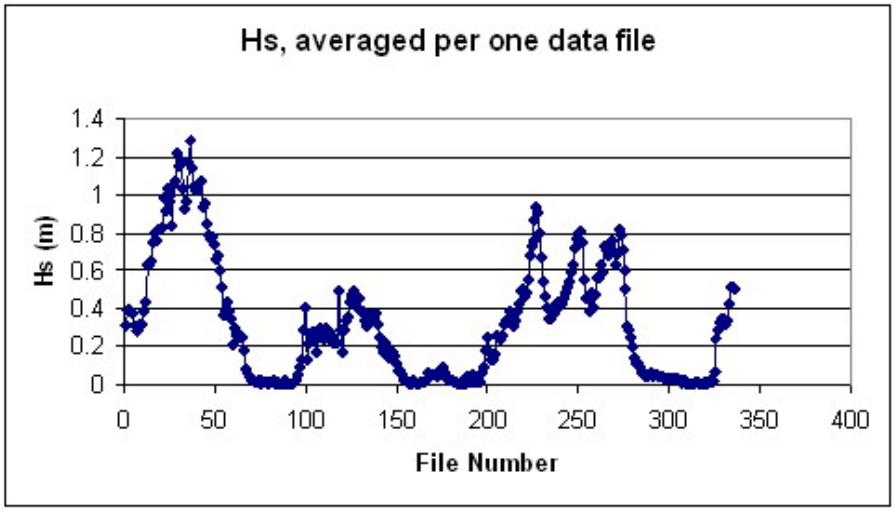

Figure 11: Sea State from the 17^{th} to the 24^{th} of November 2004

These files are less affected by large amplitude random noise, so we choose to go further in the analysis of those, which covers a large number of different sea state. So, the cleanest data have been selected, over a large number of sea state. From the file 1 to 150, 48 useful data files were fund, covering different sea conditions. Then the same analysis has been done, considering only those "good data". The results obtained are presented in figure 12.

An exponential curve fitting has been used, to have envelops for our data. The exact values taken by the fitting coefficients are not interesting here; only a global view of the behaviour is needed. This will help to understand the behaviour of the structure under a certain sea state.

Indeed, while selecting only a few "good" data files, the strain deviation calculated is quite good, and seems to be real. So, it is now possible to draw some cross section view of the considered plate, for different sea state.

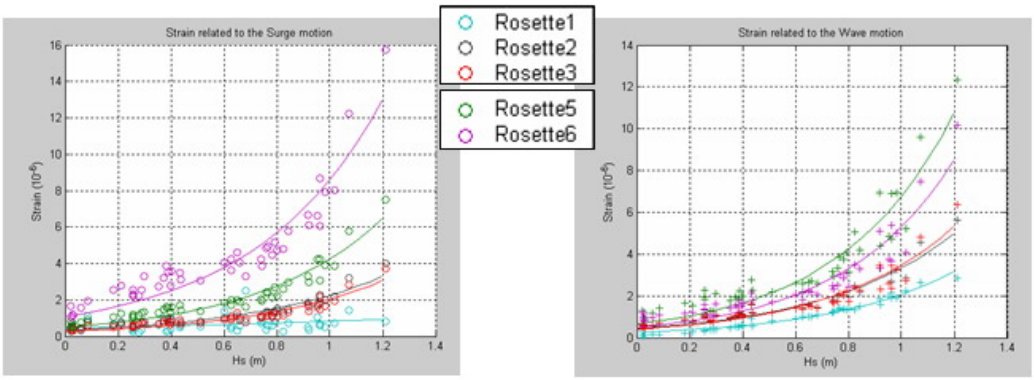

Figure 12: ϵ_{xx}obtained considering only the 48 best files

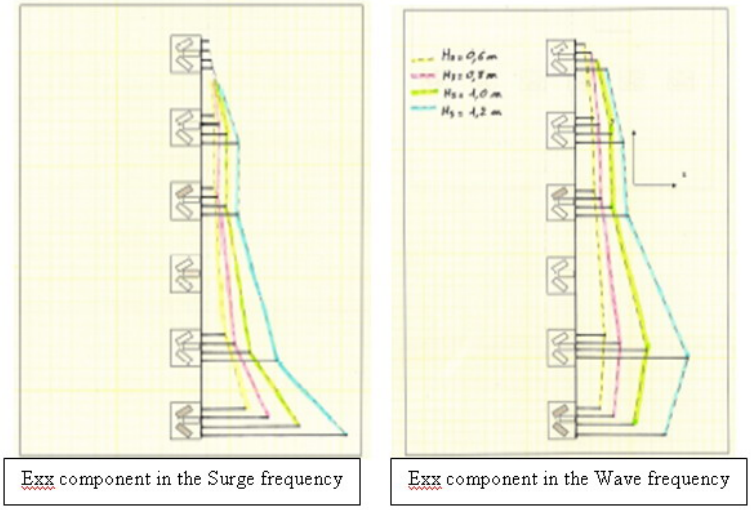

Figure 13: Cross-section of ϵ_{xx} for different wave state

Niras is a Danish partner company involved in the WD project, and in charge of the structural design (they replaced Armstrong since 01^{st} April 2005). They are also in charge of the finite element modelling of the WD Nissum Bredning prototype.

Further work is to be done to correlate the results obtained here and the FEM. Indeed, the only FE-study done today is the Ultimate Limit State study. Nevertheless, it has been possible to confirm that the overall behaviour of the FEM is confirmed by this analysis, especially by our results in the wave frequency (which are the most reliable), see Fig. 14.

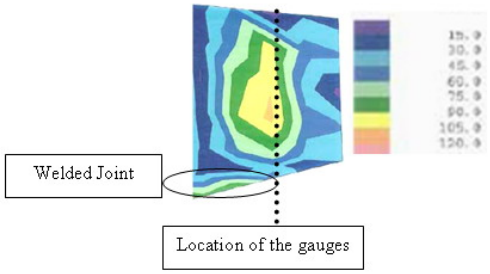

Figure 14: Von Mises stress on the vertical wall,from the ULS study [3]

Here the correlation between experimental results and FEM results is obvious, so the accuracy of the FEM is confirmed. In this drawing, it can be seen that the bottom part of the plate is a "high stress" area too. As the stress concentration factors used for the fatigue life calculation affect more the welded part, focus will be put on this bottom welded part.

PRELIMINARY FATIGUE STUDY

Reader has to bear in mind that here only a few relevant experimental results are used, so the Fatigue study that is done here is not complete at all. The lines for the future complete fatigue study are defined here, and an experimental fatigue analysis of a certain part of the main body is done. The basics of this analysis come from the *Guidelines of WEC* [2] and from the lectures and book entitled *Fatigue and Fracture Mechanics* [4].

Only three rosettes (numbered 1, 2 and 5) are available for the stress analysis, for which all the gauges of a rosette are needed to be efficient. The rosette number 5 is in the most stressed part, so those three channels will be used in this analysis.

TIME DOMAIN ANALYSIS

First of all, the average value of the signal is suppressed, because the offset values are not correctly defined for the gauges, and also several phenomena, such as the temperature, can affect this value. Moreover, it will then be possible to get back to the strains in the local coordinates, which are a linear combination of the 3 different channels.

So the strain in the local axis is calculated. Here is considered a rosette defined in Fig.3, and the appropriate formulas follow :

$$\epsilon_{xx} = Ch(B) \tag{5}$$
$$\epsilon_{yy} = Ch(A) + Ch(C) - Ch(B) \tag{6}$$
$$\epsilon_{xy} = Ch(C) - Ch(A) \tag{7}$$

As here the stresses are within the Elastic domain, the Hooks law can be used to get back to the stresses in the local coordinates :

$$\sigma_{xx} = \frac{E}{1-\nu^2}(\epsilon_{xx} + \nu\epsilon_{yy}) \tag{8}$$
$$\sigma_{yy} = \frac{E}{1-\nu^2}(\epsilon_{yy} + \nu\epsilon_{xx}) \tag{9}$$
$$\tau_{xy} = \frac{E}{2(1+\nu)}\epsilon_{xy} \tag{10}$$

Thus the stresses in the local basis are obtained, for each time step. Then, for each time step, the Von Mises equivalent stresses is calculated. It is defined as follow :

$$\sigma_{eq(VM)} = \sqrt{(\sigma_{xx} + \sigma_{yy})^2 + 3.\tau_{xy}} \tag{11}$$

The reader has to bear in mind that we are speaking here only about deviation values around the mean. So, the Von Mises equivalent stress is here the stress induced by the deviation between the average value and the present state of strain.

FREQUENCY DOMAIN ANALYSIS

For calculating the standard deviation of the Von Mises stress, we also use the FFT analysis described before. We will only focus on the component related to the wave frequency, as it will be the leading part for the fatigue design.

While assuming the stresses induced by the wave to be Rayleigh distributed, the significant stress range is estimated by using the same formula than for the significant wave height (corresponding to the average height of the 1/3 highest wave, estimated as 4 $\sqrt{m_0}$). This assumption is made to ensure the results are on the safe side. As the stress range is an amplitude, the significant stress will be defined as two times the squared root of the mo moment (related to wave frequency) of the stress spectrum.

Now the fatigue analysis that has been done will be detailed, using the previous results. The fatigue analysis intended here is very simplified, and the accuracy of the results obtained is quite low. Indeed, it is assume that the stress range obtained for the rosette 5 is the same than in the welded joint, in the bottom of the wall. Due to the FEM simulation done by Niras (see Fig.14), we can see that we overestimate the stress range value, so that the Design Fatigue Factors (DFF) we will obtain will be underestimate.

The results obtained are assumed to be on the safe-side, so it will give an order of magnitude for the fatigue life cycle of this part of the main body. As the shoulder part is considered to be the weakest part of the WD, those results will be good information. A limit of this analysis is the FEM simulation. Indeed, the other part of the shoulder of the main body is more stressed in the FEM results, but there are no gauges on this wall, see [3].

RELATION BETWEEN SEA STATE AND STRESS RANGE

The values obtained for the Von Mises equivalent stresses are amplitude deviation values. While considering the mo moment in the wave frequency (from 0.1 to 1 Hz roughly corresponding to a third and three times the wave period Tp), the stress range is defined, related to one 30 minutes data file. So, this stress range can be related to the significant wave height. Curve for the rosette 5 is shown in Fig. 15.

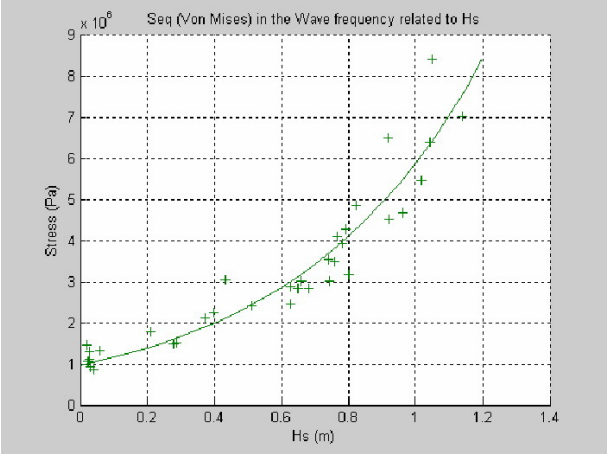

Figure 15: σ_{eq} Von Mises, rosette 5

DEFINITION OF THE K FACTORS

As it was said before, the stress range measured here is assumed to be the same than the one affecting at the bottom welded joint. According to the FEM, this assumption is on the safe side. According to the *Guidelines on design and operation of WEC* [2], the K factor obtained is 2 (Fig. 16). As the wall thickness is less than 25 mm, there is no correction induced by the thickness, and $K_t = 1$.

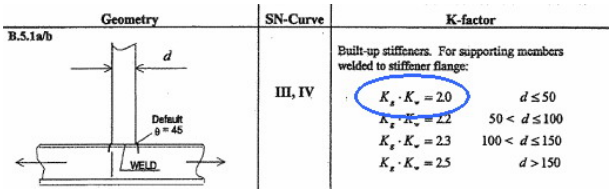

Figure 16: K factor defined by the *Guidelines of WEC*

DEFINITION OF THE LONG TERM LOADING

Here the long stress loading is assumed as being induced by the historical wave height given in table 1. This table is issued from JP Kofoed and al, *Hydraulic Response of the Wave Energy Converter Wave Dragon in Nissum Bredning* [1]. It represents the value obtained trough a two month measurement, taking place during the autumn. As it can be seen in the above mentioned paper, considering these values as the long term distribution is on the safe side. Only a few parts of the data files are registered efficiently and this analysis only focus on a little part of our database, so it is impossible to use a Rainflow counting technique for our data.

Hs	Pourcentage Occurence
0.05	33.1
0.15	12.4
0.25	8.8
0.35	12.7
0.45	9.2
0.55	7.4
0.65	5.1
0.75	4.7
0.85	3.3
0.95	1.9
1.05	0.7
1.15	0.4
1.25	0.1
1.35	0.2
1.45	0

Table 1: Historical Loading in NB

SN CURVE FOR THE CONSIDERED STEEL

The steel considered here is a Grade A steel, with a yield strength of 235 MPa. The generic SN equation for this steel is the following :

$$\sigma_d(N_{cycle}) = 925 \times N_{cycle}^{-0.12} \tag{12}$$

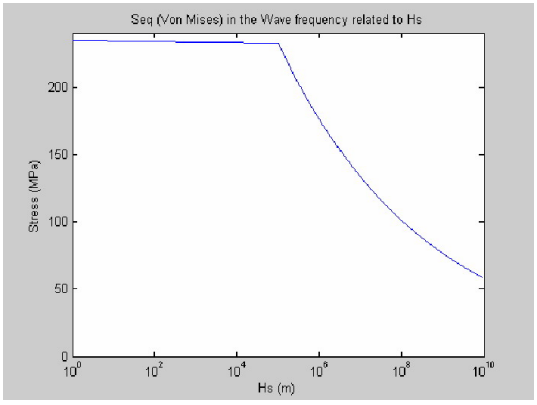

Figure 17: SN curve for the considered steel

MINER'S RULE

Miner's rule is to be used when the historical fatigue loading include several stress ranges, witch is the case when speaking of wave induced stresses on WEC. This is a linear combination rule for the different loading. The miner's rule is used for alternate stress range.

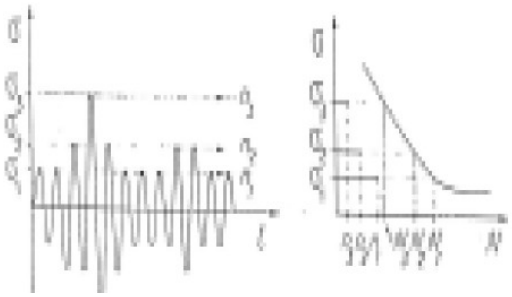

Figure 18: Graphic explaination of Miner's rule

Miner's rule definition :

$$\Sigma \frac{n_i}{N_i} = \frac{n_1}{N_1} + \frac{n_2}{N_2} + \frac{n_3}{N_3} \leq 1 \tag{13}$$

Where n_i is the number of cycle for the stress range i, assuming a certain *long term loading*, while N_i is the maximum number of cycle for the stress range i, regarding the given *SN curve*.

RESULTS OBTAINED TROUGH THIS ANALYSIS

It is important to say an other time that the results obtained here are just information, ad in no way used for any design purpose. This analysis is just a first draw of the fatigue study that has to be done for the Wave Dragon. The Fig. 17 presents the relation the DFF and the probability of failure, considering a 20 year life cycle.

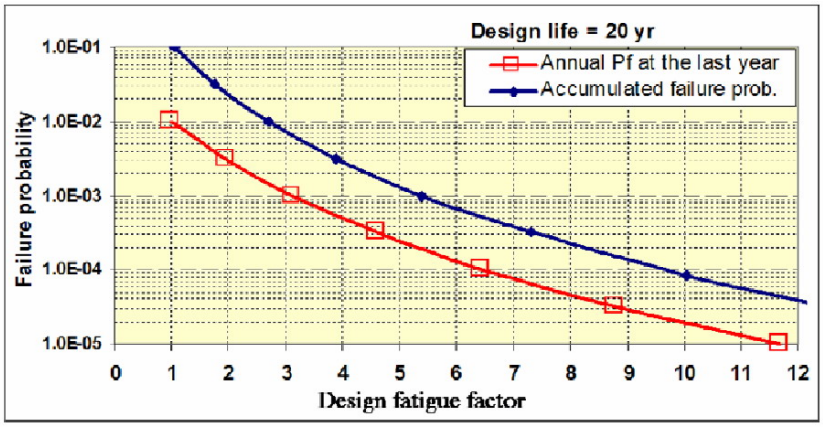

Figure 19: Failure probability as a function of the DFF, given by [2]

According to this graph, the accumulated failure probability of this part of the Wave Dragon, regarding fatigue life, is roughly 1.0E-03. As it was expected, the strategy chosen by Armstrong (the company that was in charge of the design of the WD Nissum Bredning prototype) has been to overestimate the design, and this experimental fatigue analysis confirms this overestimation.

Hs	0.05	0.15	0.25	0.35	0.45	0.55	0.65	0.75	0.85	0.95	1.05	1.15	1.25	1.35
Pourcentage Occurence	33.1	12.4	8.8	12.7	9.2	7.4	5.1	4.7	3.3	1.9	0.7	0.4	0.1	0.2
K.S (Hs) = K.A exp (b.Hs)	2,122,698	2,541,331	3,042,526	3,642,565	4,360,941	5,220,995	6,250,666	7,483,406	8,959,263	10,726,185	12,841,575	15,374,157	18,406,208	22,036,231
Ni (S) = (S/So)^(-1/b)	4.92E+15	9.58E+14	1.87E+14	3.63E+13	7.07E+12	1.38E+12	2.68E+11	5.22E+10	1.02E+10	1.98E+09	3.85E+08	7.50E+07	1.46E+07	2.84E+06
N_cycle	2.00E+08													
ni = P_occ.N_cycle	6.62E+07	2.48E+07	1.76E+07	2.54E+07	1.84E+07	1.48E+07	1.02E+07	9.40E+06	6.60E+06	3.80E+06	1.40E+06	8.00E+05	2.00E+05	4.00E+05
ni / Ni	1.34E-08	2.59E-08	9.43E-08	6.99E-07	2.60E-06	1.07E-05	3.81E-05	1.80E-04	6.50E-04	1.92E-03	3.64E-03	1.07E-02	1.37E-02	1.41E-01
Σ ni / Ni	1.72E-01													
DFF	**6**													

Table 2: Results from the FLS

ACKNOWLEDGEMENT

In this paper, the strain distribution, in terms of deviation of xx, has been correlated with the sea state. The strains measured have been divided in a long periodic part (portion of the spectrum relatives to the surge frequency, 0.01 Hz) and in a wave induced part (portion of the spectrum relatives to the wave frequency, 0.3 Hz). Then cross-sections of the considered wall have been drawn, for different sea states.

This result was then compared with the results obtained from the FEM. It has been seen to there is a good correlation in the overall behavior of these two results, even if it was not possible to correlate the values. Further work is to be done to calibrate the FEM model with the experimental results coming from the different strain gauges.

A preliminary experimental fatigue study has also been made. From this, it has been shown that the considered part of the Wave Dragon is safe designed regarding the fatigue analysis. Further investigations have to be made, combining the FEM results and experimental results, to redefine more exactly the different hot spots, and the range of stress acting in those parts. Then a complete fatigue study of the Wave Dragon prototype will be possible.

REFERENCES

[1] : JP Kofoed and P Frigaard, Aalborg University, DK : *Hydraulic Response of the Wave Energy Converter Wave Dragon in Nissum Bredning*,2004

[2] : Det Norske Veritas, commissioned by Carbon Trust : *Guidelines on design and operation of wave energy converter*, 2005

[3] : Niras, SiH/KHP, DK : *Wave Dragon 1:4,5 Workpackage 2.5 - deliverable 32 and 35, Structural finite element modeling of the Wave Dragon*, 2006

[4] : XJ Gong : lectures and book on *Fatigue and Fracture Mechanics*, I.S.A.T., Nevers, Fr, 2005

[5] : JP Kofoed, Aalborg University,DK : *Instrumentering af Wave Dragon, Nissum Bredning*